Insight into the photocatalytic mechanism of the optimal *x* value in $BiOBr_xI_{1-x}$, $BiOCl_xI_{1-x}$ and $BiOCl_xBr_{1-x}$ series varying with pollutant type

Ruixin Lu, Abdul Hannan Zahid, Qiaofeng Han*

Key Laboratory for Soft Chemistry and Functional Materials, Ministry of Education, Nanjing University of Science and Technology, Nanjing 210094, China

Figure S1 EDS spectra of $BiOBr_{0.5}I_{0.5}$ (a) and $BiOBr_{0.95}I_{0.05}$ (b)

Table S1 Apparent rate constant (*k*) of MG photodegradation on $BiOBr_xI_{1-x}$ with different *x* values

x values	0	0.05	0.25	0.4	0.5
k (min^{-1})	0.01286	0.01634	0.01803	0.02050	0.03145
x values	0.6	0.75	0.875	0.95	1
k (min^{-1})	0.01871	0.01723	0.01060	0.00661	0.00630

Table S2 Apparent rate constant (*k*) of TC photodegradation on $BiOBr_xI_{1-x}$ with different *x* values

x values	0	0.05	0.25	0.4	0.5
k (min^{-1})	0.00251	0.00452	0.00582	0.00735	0.01096
x values	0.6	0.75	0.875	0.95	1
k (min^{-1})	0.01193	0.02535	0.03283	0.03739	0.01048

* Corresponding author. E-mail: hanqiaofeng@njust.edu.cn (Q. Han).

Figure S2 Photocatalytic activity of $BiOBr_xI_{1-x}$ for the degradation of 20 mg L^{-1} TC (a), 10mg L^{-1} BPA (b), 10mg L^{-1} MV (c) and 20 mg L^{-1} RhB (d) under visible light irradiation

Figure S3 Photocatalytic activity of $BiOCl_xBr_{1-x}$ for the degradation of 20 mg L^{-1} TC (a), 20 mg L^{-1} RhB (b), 20 mg L^{-1} MG (c) and 20 mg L^{-1} MV (d) under visible light irradiation

Figure S4 Photocatalytic activity of $BiOCl_xI_{1-x}$ for the degradation of 20 mg L^{-1} RhB (a), 20 mg L^{-1} TC (b), 30 mg L^{-1} MG (c) and 20 mg L^{-1} MV (d) under visible light irradiation

Figure S5 Time-resolved spectral changes of TC (a), RhB (b) and MG (c) over $BiOBr_xI_{1-x}$

Table S3 Equilibrium adsorption capacity (q_e) for MG adsorption by fresh and used $BiOBr_xI_{1-x}$

x values	0	0.25	0.5	0.75	0.95	1
q_e (Fresh, mg g^{-1})	32	35	29	28	25	21
q_e (Used, mg g^{-1})	20	21	19	16	14	13

Table S4 Equilibrium adsorption capacity (q_e) for TC adsorption by fresh and used $BiOBr_xI_{1-x}$

x values	0	0.25	0.5	0.75	0.95	1
q_e (Fresh, mg g^{-1})	15	20	27	28	26	23
q_e (Used, mg g^{-1})	5	11	18	19	18	14

Fig. S6 Photocatalytic activity of fresh $BiOBr_xI_{1-x}$ and $BiOBr_xI_{1-x}$ after desorption for the degradation of 20 mg L^{-1} MG (a) and 20 mg L^{-1} TC (b)

Fig. S7 Effect of contact time on the removal of 20 mg L^{-1} MG (a, b) and 20 mg L^{-1} TC (c, d) over fresh $BiOBr_xI_{1-x}$ (a, c) and used $BiOBr_xI_{1-x}$ (b, d)

Figure S8 Recycling experiments of TC and MG on $BiOBr_{0.95}I_{0.05}$ and $BiOBr_{0.5}I_{0.5}$, respectively

Figure S9 XRD pattern of $BiOBr_{0.5}I_{0.5}$ (a) and (b) $BiOBr_{0.95}I_{0.05}$ before and after cycles

Figure S10 Active species trapping experiments of 20 mg L^{-1} TC photodegradation over $BiOBr_{0.95}I_{0.05}$ under visible light irradiation

Figure S11 NBT transformation efficiency on BiOI, $BiOBr_{0.5}I_{0.5}$, $BiOBr_{0.95}I_{0.05}$ and BiOBr under visible light irradiation

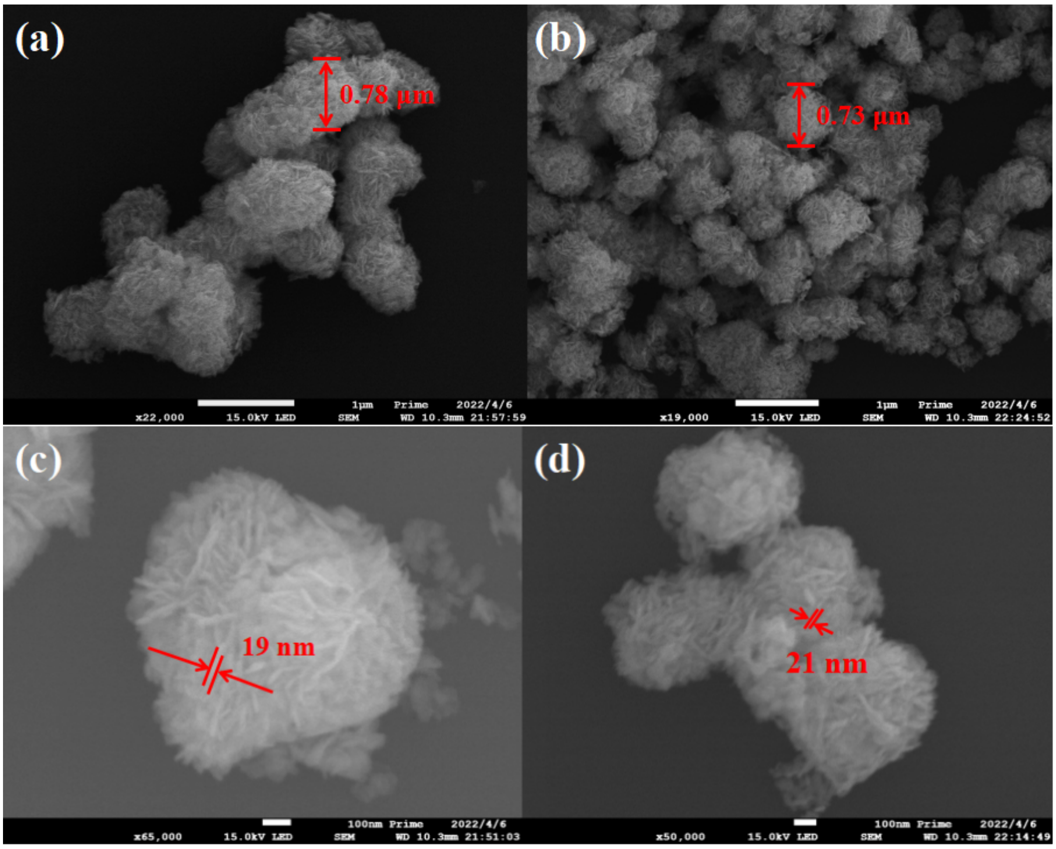

Figure S12 SEM images of $BiOBr_{0.5}I_{0.5}$ (a, c) and $BiOBr_{0.95}I_{0.05}$ (b, d)

Fig. S13 N_2 adsorption-desorption isotherms of $BiOBr_{0.25}I_{0.75}$ (a), $BiOBr_{0.5}I_{0.5}$ (b), $BiOBr_{0.75}I_{0.25}$ (c) and $BiOBr_{0.95}I_{0.05}$ (d), insets showing the corresponding pore size distribution curves and calculated surface areas and mean pore diameters

Fig. S14 Plots of Δ(pH) vs. pH measured for $BiOBr_{0.25}I_{0.75}$ (a), $BiOBr_{0.5}I_{0.5}$ (b), $BiOBr_{0.75}I_{0.25}$ (c) and $BiOBr_{0.95}I_{0.05}$ (d)

Figure S15 Mott-Schottky curves of $BiOBr_{0.95}I_{0.05}$ at different frequency (a) and $BiOBr_xI_{1-x}$ samples with different x values (b)

Figure S16 UV-vis diffuse reflectance spectra (DRS) and the plots of the $(\alpha h\upsilon)^{1/2}$ vs. photon energy ($h\upsilon$) of $BiOCl_{0.25}Br_{0.75}$, $BiOCl_{0.75}Br_{0.25}$ (a) and $BiOCl_{0.25}I_{0.75}$, $BiOCl_{0.8}I_{0.2}$ (b)

Figure S17 Mott-Schottky curves of $BiOCl_{0.25}Br_{0.75}$, $BiOCl_{0.75}Br_{0.25}$ (a) and $BiOCl_{0.25}I_{0.75}$, $BiOCl_{0.8}I_{0.2}$ (b)

Table S5 The fitting values of each component in the equivalent circuit diagram

x values	0	0.5	0.95	1
$R_1(\Omega)$	29.13	8.766	13.41	16.43
$R_2(\Omega)$	10334	2116	779.2	3694
CPE-T	3.94E-5	2.2E-3	1.64E-4	6.9E-4
CPE-P	0.86	0.35	0.71	0.79

Table S6 The band potentials and band gap energy of $BiOCl_{0.25}Br_{0.75}$, $BiOCl_{0.75}Br_{0.25}$ $BiOCl_{0.25}I_{0.75}$ and $BiOCl_{0.8}I_{0.2}$

Samples	E_g (eV)	E_{CB} (V)	E_{VB} (V)
$BiOCl_{0.25}Br_{0.75}$	2.48	-0.57	1.91
$BiOCl_{0.75}Br_{0.25}$	2.89	-0.61	2.28
$BiOCl_{0.25}I_{0.75}$	1.97	-0.18	1.79
$BiOCl_{0.8}I_{0.2}$	2.29	-0.11	2.18

Figure S18 Band structures of $BiOCl_{0.25}I_{0.75}$, $BiOCl_{0.8}I_{0.2}$, $BiOCl_{0.25}Br_{0.75}$, $BiOCl_{0.75}Br_{0.25}$ and the oxidation potential of MG, MV, TC and RhB